

Manuscript Number: EGY-D-15-02002R1

Title: Modelling the performance parameters of a horizontal falling film absorber with aqueous (lithium, potassium, sodium) nitrate solution using artificial neural networks

Article Type: Full Length Article

Keywords: triple-effect absorption cooling cycle  
horizontal falling film absorber  
aqueous nitrate solution  
alkitrate  
artificial neural network

Corresponding Author: Prof. Mahmoud Bourouis, Ph.D.

Corresponding Author's Institution: Rovira i Virgili University

First Author: María E. Álvarez, PhD

Order of Authors: María E. Álvarez, PhD; José A. Hernández, PhD; Mahmoud Bourouis, Ph.D.

Abstract: An artificial neural network (ANN) model was developed to determine the efficiency parameters of a horizontal falling film absorber at operating conditions of interest for absorption cooling systems. The aqueous nitrate solution  $\text{LiNO}_3 + \text{KNO}_3 + \text{NaNO}_3$  was used as a working fluid. The authors created the ANN from the database they had compiled with the results of experiments that they had performed in a set-up designed and built for this purpose. The ANN structure consisted of 6 input variables: inlet solution and cooling water temperatures, cooling water and solution mass flow rates, absorber pressure and inlet solution concentration; 4 output variables which facilitated the assessment of the performance of the absorber : heat and mass transfer coefficients, absorption mass flux and the degree of subcooling of the solution leaving the absorber. The hidden layer contained 9 neurons which were determined by training and test procedures. The results showed that the deviation between the experimental data and the estimated values was well adjusted. This indicated that the ANN model was an effective tool for predicting the efficiency parameters of the absorber. The solution flow rate was also observed to be the most significant operating variable which affected the performance of the absorber.

1 **Modelling the performance parameters of a horizontal falling**  
2 **film absorber with aqueous (lithium, potassium, sodium)**  
3 **nitrate solution using artificial neural networks**

4 María E. Álvarez<sup>a</sup>, José A. Hernández<sup>b</sup>, Mahmoud Bourouis<sup>a,\*</sup>

5 <sup>a</sup> *Department of Mechanical Engineering, Universitat Rovira i Virgili, Av. Països Catalans No. 26, 43007 Tarragona, Spain*

6 <sup>b</sup> *Centro de Investigación en Ingeniería y Ciencias Aplicadas, Universidad Autónoma del Estado de Morelos (UAEM), Av. Universidad*  
7 *No. 1001, Col. Chamilpa, Cuernavaca, Morelos C.P. 62209, México*

8

9 **Abstract**

10 An artificial neural network (ANN) model was developed to determine the efficiency parameters of a  
11 horizontal falling film absorber at operating conditions of interest for absorption cooling systems. The  
12 aqueous nitrate solution  $\text{LiNO}_3+\text{KNO}_3+\text{NaNO}_3$  with salt mass percentages of 53%, 28% and 19%,  
13 respectively, was used as a working fluid. The authors created the ANN from the database they had  
14 compiled with the results of experiments that they had performed in a set-up designed and built for  
15 this purpose. The ANN structure consisted of 6 input variables: inlet solution and cooling water  
16 temperatures, cooling water and solution mass flow rates, absorber pressure and inlet solution  
17 concentration; 4 output variables which facilitated the assessment of the performance of the  
18 absorber : heat and mass transfer coefficients, absorption mass flux and the degree of subcooling of  
19 the solution leaving the absorber. The hidden layer contained 9 neurons which were determined by  
20 training and test procedures. The results showed that the deviation between the experimental data

---

\* Corresponding author. Tel.: +34 977 55 86 13; Fax: +34 977 55 96 91  
Email address: [mahmoud.bourouis@urv.cat](mailto:mahmoud.bourouis@urv.cat)

21 and the estimated values was well adjusted. This indicated that the ANN model was an effective tool  
22 for predicting the efficiency parameters of the absorber. The solution flow rate was also observed to  
23 be the most significant operating variable which affected the performance of the absorber.

24

25 **Keywords:** triple-effect absorption cooling cycle, horizontal falling film absorber, aqueous nitrate  
26 solution, alkylate, artificial neural network.

27

## 28 **Highlights**

29 • An ANN model was developed for predicting the efficiency parameters of a falling film absorber  
30 working with an aqueous nitrate solution.

31 • The ANN model was created from a database compiled from experiments carried out at the  
32 operating conditions of a triple-effect absorption cooling cycle.

33 • The results indicate that the ANN model effectively predicts the efficiency parameters of falling  
34 film absorbers.

35 • The solution flow rate is the operating variable that most affects the performance of the absorber.

36

37

38 **Nomenclature**

39	$a_{\text{exp}}$	Experimental value (target)
40	$a_{\text{sim}}$	Value obtained from the simulation with the neural network
41	$b$	Intercept in the slope-intercept statistical test
42	$b_1$	Bias vector of the ANN input layer
43	$b_2$	Bias vector of the ANN output layer
44	COP	Coefficient of performance
45	$h_s$	Falling film heat transfer coefficient ( $\text{W}\cdot\text{m}^{-2}\cdot\text{C}^{-1}$ )
46	$i$	Counter of the number of data
47	$I$	Total number of input variables to the ANN
48	IR	Relative influence of an input variable on the output variable of the ANN (%)
49	IW	Matrix weight of the ANN hidden layer
50	$J$	Total number of neurons in the hidden layer
51	$k_m$	Overall mass transfer coefficient ( $\text{m}\cdot\text{s}^{-1}$ )
52	LW	Matrix weight of the ANN hidden layer
53	$m$	Slope in the slope-intercept statistical test
54	$m_{\text{abs}}$	Absorption mass flux ( $\text{kg}\cdot\text{s}^{-1}\cdot\text{m}^{-2}$ )
55	$m_c$	Cooling water flow rate ( $\text{kg}\cdot\text{s}^{-1}$ )
56	$N$	Number of data
57	$P_{\text{abs}}$	Absorber operating pressure (kPa)
58	$P_i$	Normalized input variable

- 59  $r^2$  Linear regression coefficient
- 60 rmse root mean square error
- 61  $T_{c,in}$  Cooling water temperature at the absorber entrance ( $^{\circ}\text{C}$ )
- 62  $T_{s,in}$  Solution temperature at the absorber entrance ( $^{\circ}\text{C}$ )
- 63  $x_{s,in}$  Solution concentration in salts at the absorber entrance (mass fraction)

64

65 **Greek letters**

- 66  $\Delta T_{\text{sub,out}}$  Degree of sub-cooling of the solution leaving the absorber ( $^{\circ}\text{C}$ )
- 67  $\Gamma$  Solution mass flow rate per unit of wetted tube ( $\text{kg}\cdot\text{m}^{-1}\cdot\text{s}^{-1}$ )

68

69 **Subscripts**

- 70  $I$  Number of neurons in the inlet layer
- 71  $\text{Inf}$  Lower limit
- 72  $J$  Number of neurons in the hidden layer
- 73  $K$  Number of neurons in the output layer
- 74  $\text{min}$  Minimum value
- 75  $\text{max}$  Maximum value
- 76  $\text{sup}$  Upper limit

77

78

79 **1. Introduction**

80 Recent research works reported on absorption cooling systems focus on improving the coefficient of  
81 performance (COP) by using advanced cycle configurations and compact equipment. Triple-effect  
82 absorption cooling cycles represent a substantial improvement in performance when compared with  
83 double-effect absorption cycles. Nevertheless, triple-effect cycles face more difficulties with working  
84 fluids and construction materials because they need to support temperatures of over 180°C. Álvarez  
85 et al. [1] developed a simulation model for the triple-effect absorption cooling cycle called “Alkitrato  
86 topping cycle” shown in Figure 1. The triple-effect cycle consists of a parallel double-effect cycle with  
87 H<sub>2</sub>O/LiBr as a working fluid and a single-effect cycle with an aqueous nitrate solution as a working  
88 fluid. These are coupled through the heat exchanged between external streams. The aqueous nitrate  
89 solution composed of LiNO<sub>3</sub>, KNO<sub>3</sub>, NaNO<sub>3</sub> with mass percentages of 53%, 28% and 19%,  
90 respectively, was used. Davidson and Erickson [2] proposed the use of this mixture as a working  
91 fluid in absorption chillers driven by high temperature heat sources. Later, Erikson and Howe [3]  
92 called this working fluid “Alkitrato”.

93 The absorber is usually the largest component in absorption cooling systems. An improvement in the  
94 absorption process leads to a reduction in area of the heat exchangers, and therefore a significant  
95 reduction in the costs of absorption chillers. For this reason, many researchers have focused their  
96 theoretical and experimental studies on the simultaneous processes of heat and mass transfer which  
97 take place in the absorber. In those absorption cooling systems which use water as a refrigerant and  
98 a non-volatile substance as an absorbent, the falling film absorber is generally the most frequently  
99 used design. This is because it achieves high values of heat and mass transfer coefficients in the  
100 falling film region of the solution and the pressure drop values are acceptable for the pressure  
101 conditions of this equipment. Therefore, many experimental investigations focus on falling film  
102 absorbers with horizontal tubes and most use H<sub>2</sub>O/LiBr as a working fluid.

103 The most complex aspect of the study of absorbers is the heat and mass transfer processes which  
104 occur simultaneously and are interdependent. One of the main difficulties encountered in developing  
105 a mathematical model for the absorption process is the definition of the boundary conditions at the  
106 liquid-vapour interphase. The thermal effects associated with mass transfer during the absorption  
107 process also affect the pressure, the concentration and in turn the mass transfer. Some authors  
108 proposed the use of experimental correlations to describe heat and mass transfer processes. These  
109 correlations require the calculation of dimensionless numbers, the type of equation that defines the  
110 relation between these parameters and finally an analysis of the regression between the variables  
111 [4]. It is obvious that the proposal of a precise correlation for heat and mass transfer would require  
112 an appropriate selection of the driving force for the temperature and concentration profiles [4].

113 In this work, the authors developed a model to predict the efficiency parameters of a falling film  
114 absorber with horizontal tubes, which uses the aqueous solution of  $\text{LiNO}_3+\text{KNO}_3+\text{NaNO}_3$  as a  
115 working fluid. This predictive model describes the absorber from a global perspective in order to  
116 avoid any uncertainties in local variations of temperature and concentration at the interface that need  
117 to be taken into consideration when using an analytical or semi-empirical model. Artificial Neural  
118 Networks (ANN) are promising alternative modelling tools which belong to the group of models with  
119 the black-box approach, where the estimated parameters do not need either physical interpretation  
120 nor mathematical description of the phenomena involved in the process. The ability of ANN to  
121 recognize and reproduce cause-effect relationships for multiple inputs and/or outputs by training  
122 means that they are an efficient model to represent complex systems [5].

123 The model developed in the present work incorporates the experimental database obtained from the  
124 doctoral thesis of Álvarez [6] which was carried out to characterize the process of water-vapour  
125 absorption in a falling film of an aqueous nitrate solution at operating conditions of absorption cooling  
126 cycles driven by high temperature heat sources. To predict the parameters of heat and mass transfer  
127 processes, the ANN model uses, mass flow rates, temperatures, solution concentration and

128 absorber pressure as input variables. In addition, this study provides the correlations for the  
129 parameters that define complex heat and mass transfer processes by using the minimum number of  
130 inlet parameters. This makes it easier to predict the behaviour of the absorber. The correlations were  
131 validated using the experimental database developed in the doctoral thesis of Álvarez [6].

132

## 133 **2. Application of the artificial neural network (ANN) method in absorption cooling systems**

134 The following is a brief description of the most significant studies available in literature regarding the  
135 use of the artificial neural network method in absorption cooling systems and the prediction of  
136 thermophysical properties of the working fluids used in these systems.

137 Kalogirou [7] presented a diversity of neural network applications which were mainly for renewable  
138 energy systems. In this study, the author used ANNs to model and to predict the performance of  
139 solar water heating systems, photovoltaic systems, solar radiation and wind speed. ANNs were also  
140 studied to estimate heating loads for buildings, to predict the airflow in a room with natural ventilation  
141 and the energy consumption in a passive solar energy building. The errors reported in these models  
142 were found to be within acceptable limits, clearly suggesting that ANNs can indeed be used to model  
143 renewable energy systems.

144 Chow et al. [8] introduced the use of a new concept in the control system of absorption chillers which  
145 involved integrating artificial neural networks with genetic algorithms. Fuel and energy costs incurred  
146 in the operation of direct fired absorption cooling systems were reduced globally using this concept.

147 Yang et al. [9] presented an ANN application system to control energy consumption in buildings. The  
148 study developed an optimised ANN model to determine the best time of day at which to operate the  
149 heating system in a building.

150 Sözen and Akcayol [10] used the ANN approach to analyse the performance of an absorption  
151 cooling cycle with an ejector activated by solar energy. As input variables, the model uses only the

152 operation temperatures of the four main components to predict chiller performance. The results  
153 showed that the artificial neural networks are an efficient method to predict the performance  
154 parameters of the system.

155 Another study reported by Manohar et al. [11] applied the ANN method to model a double-effect  
156 absorption chiller. The neural network was trained using experimental data and went on to predict  
157 the cooling capacity of the double-effect absorption chiller. The error margin was of  $\pm 1.2\%$  compared  
158 with the experimental data.

159 Kalogirou [12] described artificial intelligence systems (neural networks, diffuse logic, genetic  
160 algorithms and hybrid systems) applied in different renewable-energy engineering disciplines.

161 Hernández et al. [13] proposed the use of an ANN predictive model to determine the performance of  
162 a water purification process integrated into an absorption heat transformer. The model predicts on-  
163 line, the coefficient of performance (COP) and takes into account the inlet and output temperatures  
164 of each one of the four components i.e. absorber, generator, evaporator and condenser. It also  
165 considered two pressure parameters of the absorption heat transformer and the concentration of the  
166 water/LiBr solution. This model could be used in the control of the water purification process  
167 integrated into the absorption heat transformer. Later, Hernández et al. [14] developed a model of  
168 inverted artificial neural network (ANNi) to calculate the optimal operating conditions to achieve the  
169 highest COP value of the same water purification process integrated into the absorption heat  
170 transformer with a heat recovery system.

171 Labus [15] used the ANN approach, using experimental data obtained on a test bench, to obtain  
172 stationary models for low-capacity absorption refrigeration machines. The study proposed a method  
173 to control commercial absorption chillers by means of adjusting various parameters on the water side  
174 (external circuits). For this purpose, a model using experimental data was developed and a  
175 sensitivity analysis was carried out to determine which parameters most influenced the thermal loads  
176 and to optimize them further using the methodology of inverse neural network (ANNi).

177 An important field for the application of artificial neural networks is the prediction of thermodynamic  
178 and transport properties of working fluids for absorption cooling systems. There have been very few  
179 studies carried out using ANN methods to predict physical-chemical properties. Some of the studies  
180 that have used the method to predict the properties of working fluids are the following:

181 Sharma et al. [16] applied artificial neural networks (ANNs) to estimate the liquid-vapour equilibrium,  
182 using a back-propagation algorithm. Methane-ethane and ammonia-water systems were studied.  
183 Their results demonstrated the interesting possibilities of using neural networks to analyse  
184 thermodynamic mixtures.

185 Homer et al. [17] developed a method, using artificial neural networks, to predict the viscosity,  
186 density, heat of vaporization, boiling point and Pitzer's acentric factor for pure organic liquid  
187 hydrocarbons applying a wide range of temperatures. Using ANNs to predict viscosity they obtained  
188 an absolute average deviation between the estimated values and the experimental values  
189 approximately two times lower than those obtained with other predictive methods.

190 Nashawi and Elgibaly [18] developed a neural network model to predict viscosity in organic  
191 compounds. They used a set of 110 experimental data at an interval for viscosity between 0.197 and  
192 19.9 mPa.s.

193 Chouai et al. [19] applied artificial neural networks to predict pressure-volume-temperature data and  
194 other thermodynamic properties like enthalpy, entropy, compressibility factor and heat capacity of  
195 R134a, R32 y R143a refrigerants.

196 Sözen et al. [20, 21] used artificial neural networks to predict the properties of the two alternative  
197 refrigerant/absorbent couples (methanol/LiBr and methanol/LiCl) used in absorption cooling systems.  
198 The model used the back-propagation learning algorithm with three input variables, namely  
199 temperature, pressure and composition, and specific volume was considered as an output variable.

200 In order to train the neural network they used experimental data and after training they obtained an  
201 average error margin of approximately 1%.

202 Sözen et al. [22] used the artificial neural networks to determine the thermodynamic properties  
203 (specific volume, enthalpy and entropy) of an alternative refrigerant (R508b) for both the saturated  
204 liquid-vapour region and the superheated vapour region. They used the back-propagation learning  
205 algorithm and the sigmoidal transfer function. The authors showed that the ANN method reduced  
206 error in predicting property values and also eliminated the need for complex analytic equations that  
207 require long computational time and effort.

208 Sençan et al. [23] used the ANN approach to predict the enthalpy of the working fluids H<sub>2</sub>O/LiBr and  
209 H<sub>2</sub>O/LiCl used in absorption cooling systems. The study also included comparing the performance of  
210 the absorption cooling systems employing these working fluids.

211

212

### 213 3. Structure of the artificial neural network

214 Artificial neural networks are inspired by the biological process of the human brain where the  
215 neurons are interconnected to process a large quantity of information. The neural network is an  
216 adaptive system which can be trained to perform a particular function and uses the input and output  
217 information flowing through the network. An artificial neural network is made up of processing units  
218 called neurons and each network has a set of neurons grouped together in layers that inter-relate  
219 with others by means of interconnections called weights. These weights can be adjusted to model  
220 complex relationships between inputs and outputs. The first layer forming the neural network is the  
221 inlet layer, which receives information from outside (input data). The last layer is called the output  
222 layer and propagates the information from the network back to the outside. Between these layers  
223 there are one or more layers called 'hidden' layers because they are located inside the network and  
224 only exchange information with the layers adjacent to them, i.e. inlet and outlet. Each unit (neuron) in  
225 the hidden layer carries out a weighted addition of its inputs and then applies its transfer function to  
226 pass on the information from the input layer to the hidden layer. The number of neurons present in  
227 the hidden layer is determined by the required precision of the data predicted at the outlet. There is  
228 no explicit rule to determine the structure of artificial neural networks, i.e. to know the number of  
229 neurons present in the hidden layer or the number of hidden layers, so a training and test method is  
230 usually applied to find out the best structure. The response from the neurons in the hidden layer acts  
231 as input to the neurons in the output layer, producing the weighted sum and applying another  
232 transfer function.

233 The activation or transfer functions at the outlet of each neuron are the response of the network to  
234 the input that it receives. The most usual transfer function used for the hidden layer is the hyperbolic  
235 tangent sigmoid transfer function (tansig):

$$236 \quad f(x) = \frac{2}{1 + \exp(-2x)} - 1 \quad (1)$$

237 For the output layer however, the linear transfer function (purelin) is generally used:

238 
$$f(x) = x \quad (2)$$

239 The main characteristic of artificial neural networks is the capacity to learn from their environment,  
240 which means that there is a continuous improvement in their performance. With artificial neural  
241 network methodology, the data is divided into three groups: training, validation and testing. The  
242 number of neurons present in the input and output layers is, respectively, the number of variables  
243 required to make the prediction and the number of variables to be predicted [24]. The back-  
244 propagation uses an algorithm with a descending gradient which makes a comparison between the  
245 inlet to the network and the target output and iterates it until the difference reaches the value of  
246 tolerance set. The error margin is calculated as the difference between the target output value and  
247 the network output for N data, the root mean square error (rmse) is applied and is defined as:

248 
$$\text{rmse} = \sqrt{\frac{1}{N} \sum_{i=1}^N (a_{\text{sim}(i)} - a_{\text{exp}(i)})^2} \quad (3)$$

249 where  $a_{\text{sim}}$  is the value obtained from the ANN simulation,  $a_{\text{exp}}$  is the experimental value at the outlet,  
250 N is the number of data used and i is the data counter.

251

#### 252 **4. Database for the ANN model**

253 The success of obtaining a reliable and robust artificial neural network depends mainly, on the  
254 choice of the process variables involved, the data available and the domain used for training [25]. An  
255 experimental database was obtained by the authors [6] for the absorption process of water vapours  
256 in a falling film on horizontal tubes of an aqueous nitrate solution of lithium, potassium and sodium  
257 (working fluid called Alktrate). The experimental tests were carried out to characterize the absorption  
258 process with this working fluid at operating conditions of interest for triple-effect absorption cooling

259 cycles driven by high temperature heat sources. The following is a brief description of the  
260 experimental device used and the experimental database developed.

#### 261 **4.1 Description of the experimental device used to study the absorption process**

262 The experimental set-up used to characterize the absorption process of water vapour in a falling film  
263 on horizontal tubes of an aqueous nitrate solution was described in detail by Álvarez [6]. This  
264 experimental device was designed to operate under continuous steady-state mode and to register  
265 the experimental data at different operating conditions. It was composed of three main circuits: the  
266 solution fluid circuit, the cooling water circuit and the vapour circuit. The absorber is the heart of the  
267 experimental set-up and is made up of a cylindrical chamber which contains a bundle of 6 copper  
268 tubes horizontally aligned and connected in series; a solution distributor at the inlet and a solution  
269 collecting tray at the absorber exit. The nitrate solution of lithium, potassium and sodium flows over  
270 the surface of the tubes forming a falling film in counter-flow with the water vapour coming from the  
271 generator. At the absorber exit there is only a solution stream with a lower concentration in  
272 absorbent than at the entrance, because water vapour has been absorbed. The falling film formed  
273 over the surface of the absorber tubes is cooled by the cooling water flowing at a cross-flow direction  
274 with the solution inside the tubes that make up the absorber. Figure 2 shows an internal view of the  
275 absorber.

#### 276 **4.2. Operating conditions and structure of the experimental database**

277 The nominal operating conditions of the application studied here establish a mass fraction in salts of  
278 0.82 of the aqueous nitrate solution at the absorber entrance, an operating pressure of 30 kPa and  
279 an inlet cooling water temperature varying between 70 and 90°C. A study of sensitivity was carried  
280 out for the following operating variables: absorber pressure ( $P_{\text{abs}}$ ), temperature and flow rate of the  
281 cooling water entering the absorber ( $T_{\text{c,in}}$  and  $m_{\text{c}}$ , respectively), solution flow rate per unit of absorber

282 length ( $\Gamma$ ), temperature and concentration of the solution at the absorber inlet ( $T_{s,in}$  and  $x_{s,in}$ ,  
283 respectively).

284 The operating parameters of the absorber, namely  $P_{abs}$ ,  $T_{c,in}$ ,  $m_c$ ,  $\Gamma$ ,  $T_{s,in}$  and  $x_{s,in}$  were established as  
285 input variables to the neural network. A series of experiments were performed at a solution mass  
286 fraction of 0.82 with a total of 49 experimental data points. These experiments covered the range of  
287 operating conditions in a triple-effect absorption cooling cycle driven by high temperature heat  
288 sources. In this first set of data, 37 data points were obtained at an absorber pressure of 30.0 kPa  
289 and 12 data points at 35.0 kPa. Afterwards a second set of 8 experimental data points was obtained  
290 at a lower mass fraction in absorbent of 0.75. In both cases, some parameters were maintained  
291 constant while others were changed. Hence, 57 experimental data points were used to feed the  
292 neural network. The experimental database was divided into three groups: training (80%), validation  
293 (10%) and trials (10%), all of which were selected randomly from the total set of data.

294 In the artificial neural network approach, it is generally a requirement to normalize the data in the  
295 input layer to guarantee that the influence of each input variable in the model is not determined by  
296 the magnitude of its original values or by its range in variation. The normalization technique used  
297 consists in applying a linear transformation of the inputs to variables in the range [0, 1]. As the  
298 transfer function used in the hidden layer is the hyperbolic tangent sigmoid function (tansig), all  
299 inputs have been normalized within the range [0.1, 0.9] so all input data  $I_i$  was increased to a new  
300 value  $P_i$  employing the following equation [25]:

301 
$$P_i = 0.8 \left( \frac{I_i - I_{min}}{I_{max} - I_{min}} \right) + 0.1 \quad (4)$$

302 The following values were taken from the experimental database and used for the model: maximum  
303 ( $I_{max}$ ) and minimum ( $I_{min}$ ) inlet values of 35.1 kPa and 29.95 kPa for the absorber pressure ( $P_{abs}$ ),  
304 0.822 and 0.748 for the absorbent mass fraction in the solution at the absorber inlet ( $x_{s,in}$ ), 108.4 °C  
305 and 89.6 °C for the solution temperature at the absorber inlet ( $T_{s,in}$ ), 86.1 °C and 70.9 °C for the inlet

306 cooling water temperature ( $T_{c,in}$ ), 0.063 kg.s<sup>-1</sup> and 0.040 kg.s<sup>-1</sup> for the cooling water flow rate at the  
307 absorber inlet ( $m_c$ ), and 0.0213 kg.m<sup>-1</sup>.s<sup>-1</sup> and 0.0095 kg.m<sup>-1</sup>.s<sup>-1</sup> for the solution flow rate by unit of  
308 the absorber length ( $\Gamma$ ).

309

## 310 **5. Results and discussion**

311 This section presents the artificial neural network model used to determine the performance  
312 parameters of a horizontal falling film absorber that uses aqueous nitrate solution as a working fluid.  
313 The validation of the artificial neural network model with the experimental database elaborated by the  
314 authors is also reported together with the analysis of sensitivity performed to assess the variable  
315 most influential in the absorber performance.

### 316 **5.1. Artificial neural network model**

317 The calculations were carried out using Matlab software (Natick, MA, USA) and its specific  
318 application for artificial neural networks. As reported above, the following 6 input variables were  
319 selected: absorber pressure ( $P_{abs}$ ), solution temperature at the absorber inlet ( $T_{s,in}$ ), inlet cooling  
320 water temperature ( $T_{c,in}$ ), solution concentration at the absorber inlet ( $x_{s,in}$ ), inlet cooling water flow  
321 rate ( $m_c$ ) and solution flow rate by unit of absorber length ( $\Gamma$ ). For the output variables, the following  
322 four parameters that characterize the absorption process were defined: the heat transfer coefficient  
323 of the falling film ( $h_s$ ), the mass flow rate of water vapour absorbed per unit area of the absorber  
324 ( $m_{abs}$ ), the mass transfer coefficient ( $k_m$ ) and the degree of sub-cooling of the solution leaving the  
325 absorber ( $\Delta T_{sub,out}$ ). The input variables were normalized within the range [0.1, 0.9] by the equation  
326 (4). The artificial neural network model was developed in two stages. The first one involved learning  
327 and validating the network and the second, evaluating the model with the data which had not been  
328 used in the training stage (Figure 3). Training of the neural network was based on the back-  
329 propagation technique using the Levenberg-Marquardt optimization algorithm that adjusts the

330 weights and biases to minimize the error (rmse) between simulated values and experimental values  
 331 (target).

332 During the learning stage, training and test methods were used to evaluate different network  
 333 structures. The performance of each structure analysed was then evaluated with the parameters, the  
 334 root mean square error (rmse) and the linear regression coefficient ( $r^2$ ). It was observed that the  
 335 ANN structure containing nine neurons in the hidden layer was the one that obtained the best results  
 336 (minimum rmse and maximum  $r^2$ ) for predicting performance parameters of the absorber. Therefore,  
 337 the following 6-9-4 neural network structure was chosen as shown in Figure 4. An input layer  
 338 composed of 6 neurons, a hidden layer of 9 neurons and an output layer of 4 neurons. The algorithm  
 339 uses a hyperbolic tangent sigmoid transfer function (tansig) in the hidden layer and a linear transfer  
 340 function (purelin) in the output layer.

341 Finally, the ANN model for the performance parameters of the horizontal falling film absorber using  
 342 an aqueous nitrate solution as a working fluid was defined by the equation (5):

$$343 \quad a_k = \sum_{j=1}^J \left[ LW_{k,j} \frac{2}{\left( 1 + \exp \left( -2 \left( \sum_{i=1}^I IW_{j,i} P_i + b_{1j} \right) \right) \right)} - 1 \right] + b_{2k} \quad (5)$$

344 where I is the number of inputs (I=6), J is the number of neurons in the hidden layer (J=9),  $P_i$  is the  
 345 input "i" normalized, IW and LW are the weight matrix in the hidden and output layers respectively,  $b_1$   
 346 and  $b_2$  are the bias vectors in the hidden and output layers respectively, a is the output variable and  
 347 k is the number of the output variable, where k=1 refers to the output  $a_1=h_s$ , k=2 to  $m_{abs}$ , k=3 to  $k_m$   
 348 and k=4 to  $\Delta T_{sub,out}$ .

349 Table 1 shows the best adjustment in weights ( $IW_{j,i}$  and  $LW_{k,j}$ ) and biases ( $b_{1j}$  and  $b_{2k}$ ) of the neural  
 350 network structure with 9 neurons in the hidden layer (Figure 4) obtained during the learning stage of  
 351 the model developed for the performance parameters of the horizontal falling film absorber. As a

352 sample of the calculation process, the following equations were developed for the output 1 (k=1)  
 353 which corresponds to the falling film heat transfer coefficient  $h_s$  depending on the input variables, the  
 354 weights and the biases.

$$355 \quad h_s = 2 \left[ \frac{LW_{1,1}}{1 + \exp(n_1)} + \frac{LW_{1,2}}{1 + \exp(n_2)} + \frac{LW_{1,3}}{1 + \exp(n_3)} + \frac{LW_{1,4}}{1 + \exp(n_4)} + \frac{LW_{1,5}}{1 + \exp(n_5)} + \frac{LW_{1,6}}{1 + \exp(n_6)} + \frac{LW_{1,7}}{1 + \exp(n_7)} + \frac{LW_{1,8}}{1 + \exp(n_8)} + \dots \right. \\ 356 \quad \left. + \frac{LW_{1,9}}{1 + \exp(n_9)} \right] - (LW_{1,1} + LW_{1,2} + LW_{1,3} + LW_{1,4} + LW_{1,5} + LW_{1,6} + LW_{1,7} + LW_{1,8} + LW_{1,9}) + b_{2,1} \quad (6)$$

357 where,

$$358 \quad n_1 = -2[W_{1,1}P_1 + W_{1,2}P_2 + W_{1,3}P_3 + W_{1,4}P_4 + W_{1,5}P_5 + W_{1,6}P_6 + b_{1,1}] \quad (7)$$

$$359 \quad n_2 = -2[W_{2,1}P_1 + W_{2,2}P_2 + W_{2,3}P_3 + W_{2,4}P_4 + W_{2,5}P_5 + W_{2,6}P_6 + b_{1,2}] \quad (8)$$

$$360 \quad n_3 = -2[W_{3,1}P_1 + W_{3,2}P_2 + W_{3,3}P_3 + W_{3,4}P_4 + W_{3,5}P_5 + W_{3,6}P_6 + b_{1,3}] \quad (9)$$

$$361 \quad n_4 = -2[W_{4,1}P_1 + W_{4,2}P_2 + W_{4,3}P_3 + W_{4,4}P_4 + W_{4,5}P_5 + W_{4,6}P_6 + b_{1,4}] \quad (10)$$

$$362 \quad n_5 = -2[W_{5,1}P_1 + W_{5,2}P_2 + W_{5,3}P_3 + W_{5,4}P_4 + W_{5,5}P_5 + W_{5,6}P_6 + b_{1,5}] \quad (11)$$

$$363 \quad n_6 = -2[W_{6,1}P_1 + W_{6,2}P_2 + W_{6,3}P_3 + W_{6,4}P_4 + W_{6,5}P_5 + W_{6,6}P_6 + b_{1,6}] \quad (12)$$

$$364 \quad n_7 = -2[W_{7,1}P_1 + W_{7,2}P_2 + W_{7,3}P_3 + W_{7,4}P_4 + W_{7,5}P_5 + W_{7,6}P_6 + b_{1,7}] \quad (13)$$

$$365 \quad n_8 = -2[W_{8,1}P_1 + W_{8,2}P_2 + W_{8,3}P_3 + W_{8,4}P_4 + W_{8,5}P_5 + W_{8,6}P_6 + b_{1,8}] \quad (14)$$

$$366 \quad n_9 = -2[W_{9,1}P_1 + W_{9,2}P_2 + W_{9,3}P_3 + W_{9,4}P_4 + W_{9,5}P_5 + W_{9,6}P_6 + b_{1,9}] \quad (15)$$

367

368 The experimental and calculated data using the ANN model were compared to evaluate how the  
 369 model performed in the prediction of the output variables. Table 2 shows the values obtained for  
 370 rmse,  $r^2$  and Figure 5 shows the comparison between the experimental and simulated values of each  
 371 output variable ( $h_s$ ,  $m_{abs}$ ,  $k_m$  and  $\Delta T_{sub,out}$ ). The results obtained show that the experimental and

372 simulated data are well in line and this indicates that the model is effective for predicting the  
373 performance parameters of the absorber.

374 The slope-intercept statistical test was carried out to evaluate the performance of the neural network  
375 proposed. In accordance with the results obtained by Verma et al. [26] and to satisfy this statistical  
376 test, the range established between the values of the upper slope ( $m_{sup}$ ) and lower slope ( $m_{inf}$ ) must  
377 contain the value 1, and the range established between the values of the upper intercept ( $b_{sup}$ ) and  
378 the lower intercept ( $b_{inf}$ ) must contain the value 0. Table 3 shows the limits i.e. maximum and  
379 minimum values of the slopes and the intercepts. Both conditions have been satisfied and the model  
380 proposed passed the test with a confidence level of 99%.

## 381 **5.2. Validation of the artificial neural network model proposed**

382 Figure 6 shows the ability of the artificial neural network model to predict the performance  
383 parameters for a horizontal falling film absorber. It compares the results of the 4 performance  
384 parameters selected for the absorber obtained from experimental data ( $h_s$ ,  $m_{abs}$ ,  $k_m$  y  $\Delta T_{sub,out}$ ) and  
385 the values calculated from the neural network model, depending on the solution flow rate. The model  
386 effectively predicts the behaviour of the absorber depending on the input variables. Figure 6 also  
387 shows how the concentration of the solution entering the absorber affects the performance  
388 parameters of the absorber. The model corresponds well with the experimental data with respect to  
389 the disturbances occurring at the inlet. This shows how capable artificial neural networks are in  
390 simulating the behaviour of complex processes.

## 391 **5.3. Sensitivity analysis**

392 This section contains the results of a sensitivity study carried out to evaluate the relative importance  
393 of each input variable in the absorption process. The approach employed by El-Hamzaoui et al. [27],  
394 was used for the analysis of sensitivity presented in the present work and applies the following  
395 equation (Garson [28]):

396

$$IR_{i(k)} = \frac{\sum_{j=1}^J \left( \frac{|IW_{j,i}|}{\sum_{i=1}^I |IW_{j,i}|} |LW_{k,j}| \right)}{\sum_{i=1}^I \left[ \sum_{j=1}^J \left( \frac{|IW_{j,i}|}{\sum_{i=1}^I |IW_{j,i}|} |LW_{k,j}| \right) \right]} \quad (16)$$

397 where IR is the relative importance of the input variable I on the output variable k; I is the number of  
 398 input variables (I=6), J is the number of neurons in the hidden layer (J=9), and IW and LW are the  
 399 weights of the hidden and output layers, respectively. This way, the relative importance of each inlet  
 400 variable can be determined. Figure 7 shows the relative importance of each input variable on each of  
 401 the output variables calculated by the equation (16). In general, all the input variables have a  
 402 significant effect on the performance parameters of the absorber. However, the most relevant  
 403 variable is the flow rate of the solution entering the absorber ( $\Gamma$ ). The relative influence of the solution  
 404 flow rate is always above 20% for all the performance parameters of the absorber, except for the  
 405 falling film heat transfer coefficient  $h_s$ , which has a relative influence of 13.5%. It is therefore  
 406 concluded that the absorber can operate more efficiently if the solution flow rate of the horizontal  
 407 falling film is controlled. On the other hand, the lesser relative effect of the solution flow rate on the  
 408 falling film heat transfer coefficient coincides with the trend observed during the experimental study  
 409 reported by Álvarez [6]. Within the range of solution flow rates considered in this study, the falling  
 410 film heat transfer coefficient shows an asymptotic trend, so the effect of the solution flow rate on the  
 411 falling film heat transfer coefficient is not as pronounced as on other performance parameters. This is  
 412 another example of the ability of the ANN model to predict performance parameters of horizontal  
 413 falling film absorbers of absorption cooling systems.

414

415

## 416 6. Conclusions

417 Artificial neural network methodology was applied in this work to predict the performance parameters  
418 of horizontal falling film absorbers using an aqueous (lithium, potassium and sodium) nitrate solution  
419 as a working fluid. The model used 6 input variables: absorber pressure ( $P_{abs}$ ), solution temperature  
420 at the absorber inlet ( $T_{s,in}$ ), inlet cooling water temperature ( $T_{c,in}$ ), solution concentration at the  
421 absorber inlet ( $x_{s,in}$ ), inlet cooling water flow rate ( $m_c$ ) and solution flow rate by unit of absorber  
422 length ( $\Gamma$ ). As output variables, the following four parameters that characterize the absorption  
423 process were used: the heat transfer coefficient of the falling film ( $h_s$ ), the mass flow rate of water  
424 vapour absorbed per unit area of the absorber ( $m_{abs}$ ), the mass transfer coefficient ( $k_m$ ) and the  
425 degree of sub-cooling of the solution leaving the absorber ( $\Delta T_{sub,out}$ )

426 The structure of the neural network was determined by a training and test procedure and is made up  
427 of 6 inputs, 9 neurons in the hidden layer and 4 outputs. The model developed used an experimental  
428 database built up by the authors in a previous work with experiments to characterize the absorption  
429 process of water vapour in a falling film of an aqueous nitrate solution. This study provides an  
430 artificial neural network model to predict the performance parameters defining the complex heat and  
431 mass transfer processes by using the minimum number of input variables.

432 The artificial neural network performance was measured statistically by root mean square error  
433 (rmse) and linear regression coefficient ( $r^2$ ) calculations, which were carried out using the  
434 experimental values and the predictions from the model. The rmse values were: 1.183, 0.020, 0.013  
435 and 0.025 for  $h_s$ ,  $m_{abs}$ ,  $k_m$  and  $\Delta T_{sub,out}$ , respectively and the  $r^2$  values were: 0.9989, 0.9683, 0.9867  
436 and 0.9543 for  $h_s$ ,  $m_{abs}$ ,  $k_m$  and  $\Delta T_{sub,out}$ , respectively. The low rmse values and the high  $r^2$  values  
437 demonstrated the efficiency of the model to predict the output variables. The model proved to be  
438 very reliable when the slope-intercept statistical test was applied.

439 The relative importance (IR%) of each input variable to influence the performance parameters of the  
440 absorber was also evaluated in this study. In accordance with the sensitivity study carried out it was  
441 seen that: (i) all the input variables considered had a significant effect on the absorber performance  
442 parameters, (ii) The most relevant variable was the mass flow rate of the solution entering the  
443 absorber ( $\Gamma$ ). All the performance parameters of the absorber had a relative influence of over 20%,  
444 except for the falling film heat transfer coefficient  $h_s$ , which had an influence of 13.5%. This suggests  
445 that, for the absorber to operate more efficiently, the flow of the horizontal falling film must be  
446 specifically controlled.

447

#### 448 **Acknowledgements**

449 This study is part of an R&D project funded by the Spanish Ministry of Science and Innovation  
450 (ENE2007-65541/ALT). M. Álvarez acknowledges the receipt of scholarship award (BES-2008-  
451 006253) from the Spanish Ministry of Science and Innovation.

452

453 **References**

- 454 [1] Álvarez ME, Esteve X, Bourouis M. Performance analysis of a triple-effect absorption cooling  
455 cycle using aqueous (lithium, potassium, sodium) nitrate solution a working pair. *Applied Thermal*  
456 *Engineering*. 2015; 79:27–36.
- 457 [2] Davidson W, Erickson D. 260 °C Aqueous absorption working pair under development.  
458 *Newsletter IEA Heat Pump Centre*. 1986; 4:29–31.
- 459 [3] Erickson D, Howe L. Development of high-temperature absorption working pair. Winter Annual  
460 Meeting of the American Society of Mechanical Engineers. AES. 1989; 8:47–53.
- 461 [4] Miller W, Keyhani M. The correlation of coupled heat and mass transfer experimental data for  
462 vertical falling film absorption. In *Proc. ASME Advanced Energy Systems Division*. 1999; 39:177–87.
- 463 [5] Pareek V, Brungs M, Adesina A, Sharma R. Artificial neural network modelling of a multiphase  
464 photo degradation system. *Journal of Photochemistry and Photobiology A: Chemistry*. 2002;  
465 149:139–46.
- 466 [6] Álvarez ME. Theoretical and experimental study of the aqueous solution of lithium, sodium and  
467 potassium nitrates as a working fluid in absorption chillers driven by high temperature heat sources  
468 (in Spanish). PhD Thesis; Universitat Rovira i Virgili; Tarragona (Spain); 2013.
- 469 [7] Kalogirou S. Artificial neural networks in renewable energy system applications: a review.  
470 *Renewable and Sustainable Energy Reviews*. 2001; 5:373–401.
- 471 [8] Chow T, Zhang G, Lin Z, Song C. Global optimization of absorption chiller system by genetic  
472 algorithm and neural network. *Energy and Building*. 2002; 34:103–09.
- 473 [9] Yang I, Yeo M, Kim K. Application of artificial neural networks to predict the optimal start time for  
474 heating systems in buildings. *Energy Conversion and Management*. 2003; 44:2791–809.

- 475 [10] Sözen A, Akçayol M. Modelling (using artificial neural-networks) the performance parameters of  
476 a solar-driven ejector-absorption cycle. *Applied Energy*. 2004; 79: 309–25.
- 477 [11] Manohar H, Saravanan R, Renganarayanan S. Modelling of steam fired double effect vapour  
478 absorption chiller using neural network. *Energy Conversion and Management*. 2006; 47:2202–10.
- 479 [12] Kalogirou S. *Artificial intelligence in energy and renewable energy systems*. 2006. Nova Science  
480 Publishers Inc. New York.
- 481 [13] Hernández JA, Juárez-Romero D, Morales L, Siqueiros J. COP prediction for the integration of a  
482 water purification process in a heat transformer: with and without energy recycling. *Desalination*.  
483 2008; 219:66–80.
- 484 [14] Hernández JA, Bassam A, Siqueiros J, Juárez-Romero D. Optimum operating conditions for a  
485 water purification process integrated to a heat transformer with energy recycling using neural  
486 network inverse. *Renewable Energy*. 2009; 34:1084–91.
- 487 [15] Labus J. *Modelling of small capacity absorption chillers driven by solar thermal energy or waste  
488 heat*. (Doctoral thesis). Spain: Universitat Rovira i Virgili; 2013.
- 489 [16] Sharma R, Singhal D, Ghosh R, Dwivedi A. Potential applications of artificial neural networks to  
490 thermodynamics: vapor-liquid equilibrium predictions. *Computers & Chemical Engineering*. 1999;  
491 23:385–90.
- 492 [17] Homer J, Generalis S, Robson J. Artificial neural networks for the prediction of liquid viscosity,  
493 density, heat vaporization, boiling point and Pitzer's acentric factor. Part I: Hydrocarbons. *Chemical  
494 Physics*. 1999; 1:4075–81.
- 495 [18] Nashawi I, Elgibaly A. Prediction of liquid viscosity of pure organic compounds via artificial  
496 neural networks. *Petroleum Science and Technology*. 1999; 17:1107–44.

- 497 [19] Chouai A, Laugier S, Richon D. Modelling of thermodynamic properties using neural networks:  
498 Application to refrigerants. *Fluid Phase Equilibria*. 2002; 199:53–62.
- 499 [20] Sözen A, Özalp M, Arcaklioglu E. Investigation of thermodynamic properties of  
500 refrigerant/absorbent couples using artificial neural networks. *Chemical Engineering and Processing:  
501 Process Intensification*. 2004; 43:1253–64.
- 502 [21] Sözen A, Arcaklioglu E, Özalp M. Formulation based on artificial neural network of  
503 thermodynamic properties of ozone friendly refrigerant/absorbent couples. *Applied Thermal  
504 Engineering*. 2005; 25:1808–20.
- 505 [22] Sözen A, Özalp M, Arcaklioglu E. Calculation for the thermodynamic properties of an alternative  
506 refrigerant (R508b) using artificial neural network. *Applied Thermal Engineering*. 2007; 27:551–9.
- 507 [23] Şencan A, Yakut K, Kalogirou S. Thermodynamic analysis of absorption systems using artificial  
508 neural network. *Renewable Energy*. 2006; 31:29–43.
- 509 [24] Aleboyeh A, Kasiri MB, Olya ME, Aleboyeh H. Prediction of azo dye decolorization by UV/H<sub>2</sub>O<sub>2</sub>  
510 using artificial neural networks. *Dyes and pigments*. 2008; 77:288–94.
- 511 [25] Despange F, Massart D. Neural networks in multivariate calibration. *Analyst*. 1998; 123:157–  
512 178.
- 513 [26] Verma S, Mekhjian M, Sandor G, Nakada N. Corrosion inhibitor in lithium bromide absorption  
514 fluid for advanced and current absorption cycle machines. *ASHRAE Transactions*. 1999; 105:813–  
515 15.
- 516 [27] Hamzaoui Y, Hernández JA, Silva-Martínez S, Bassam A, Álvarez A, Lizama-Bahena C.  
517 Optimal performance of COD removal during aqueous treatment of alazine and gesaprim  
518 commercial herbicides by direct and inverse neural network. *Desalination*. 2011; 227:325–37.

519 [28] Garson G. Interpreting neural-network connection weights. *Artificial Intelligence Expert*. 1991;  
520 1:47-51.  
521

522 **Figures Caption**

523 Figure 1. Configuration of the triple-effect absorption cooling cycle with a high temperature Alkitate  
524 stage [1]

525 Figure 2. Internal view of the absorber employed to build the experimental database used in the ANN  
526 model

527 Figure 3. Architecture of the neural network employed to model the performance parameters of the  
528 absorber and the procedure used to train the network

529 Figure 4. Structure of the neural network employed to predict the performance parameters of the  
530 horizontal falling film absorber that uses an aqueous nitrate solution as a working fluid.

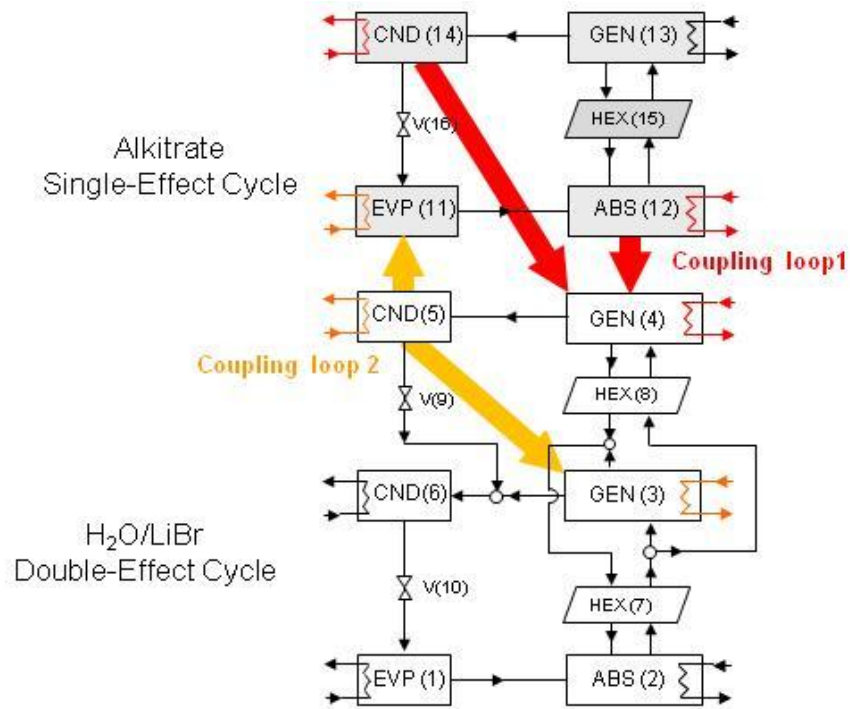
531 Figure 5. Comparison between experimental data and the values obtained using the ANN model (a)  
532 Falling film heat transfer coefficient,  $h_s$ ; (b) Absorption mass flux,  $m_{abs}$ ; (c) Mass transfer coefficient,  
533  $k_m$ ; (d) Degree of sub-cooling of the solution leaving the absorber,  $\Delta T_{sub,out}$ .

534 Figure 6. Validation of the ANN model to predict the absorber performance parameters:  $\blacklozenge$  75%  
535 (experimental data),  $\blacklozenge$  82% (experimental data),  $\_$  prediction by the neural network of: (a) Falling  
536 film heat transfer coefficient ( $h_s$ ); (b) Absorption mass flux ( $m_{abs}$ ); (c) Mass transfer coefficient ( $k_m$ );  
537 (d) Degree of sub-cooling of the solution leaving the absorber ( $\Delta T_{sub,out}$ ).

538 Figure 7. Relative importance (%) of the inlet variables on each one of the performance parameters  
539 of the absorber: (a) Falling film heat transfer coefficient ( $h_s$ ); (b) Absorption mass flux ( $m_{abs}$ ); (c) Mass  
540 transfer coefficient ( $k_m$ ); (d) Degree of sub-cooling of the solution leaving the absorber ( $\Delta T_{sub,out}$ ).

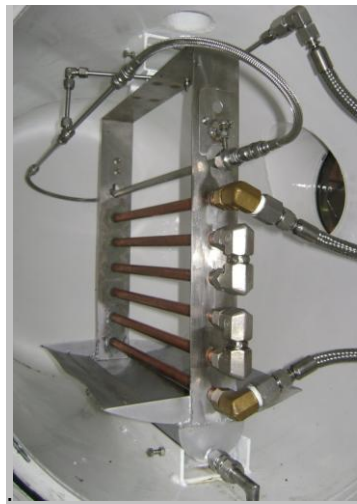
541

542



543

544 Figure 1. Configuration of the triple-effect absorption cooling cycle with a high temperature Alkitrates  
545 stage [1]

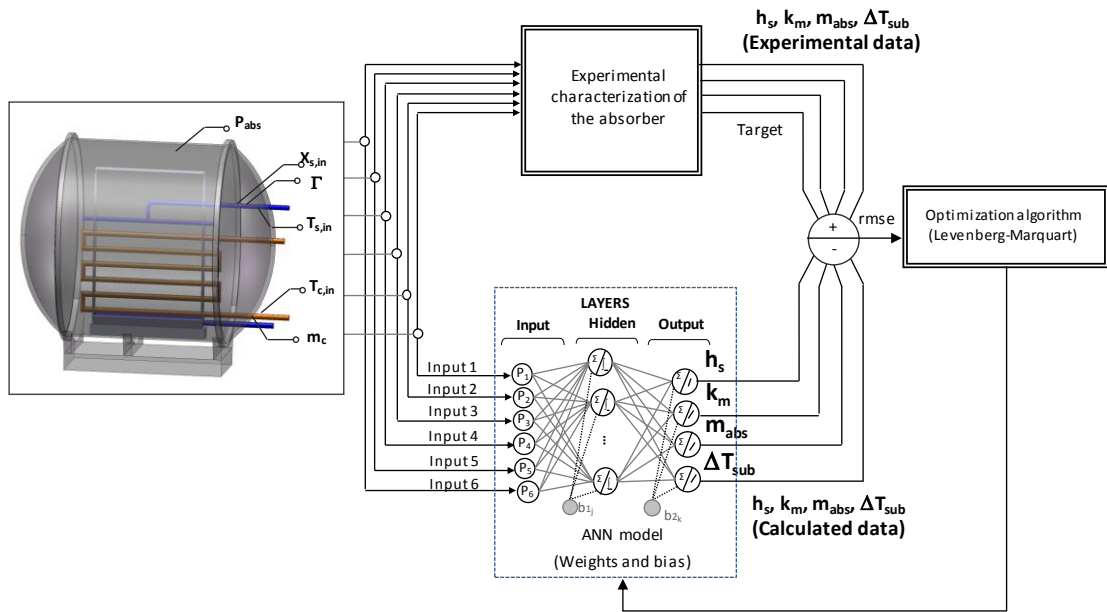


546

547 Figure 2. Internal view of the absorber employed to build the experimental database used in the ANN  
548 model

549

550

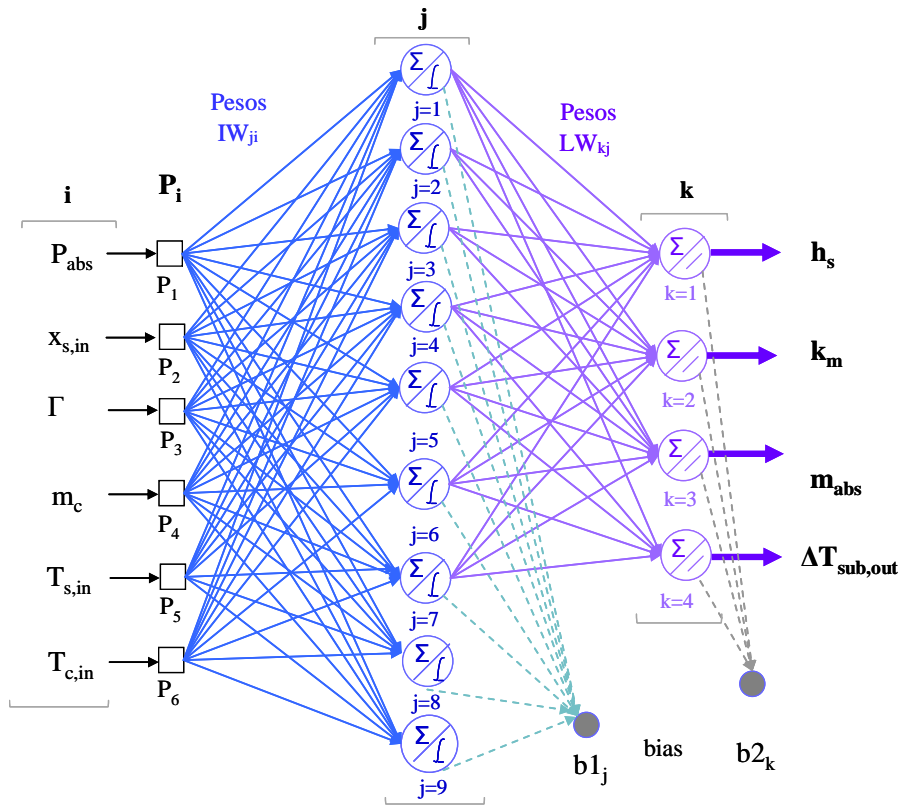


551

552 Figure 3. Architecture of the neural network employed to model the performance parameters of the  
553 absorber and the procedure used to train the network

554

555

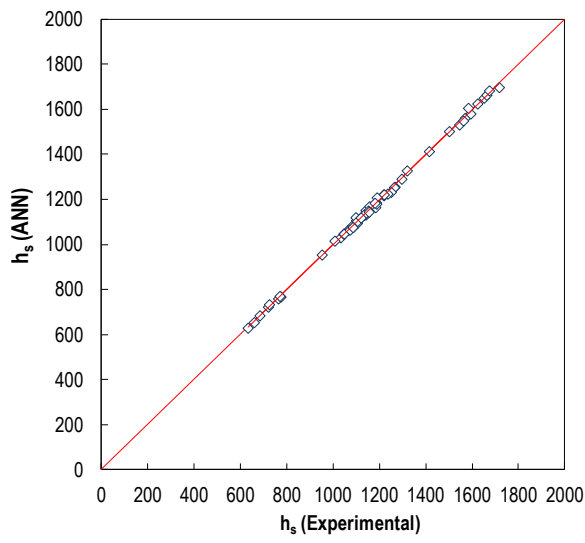


557

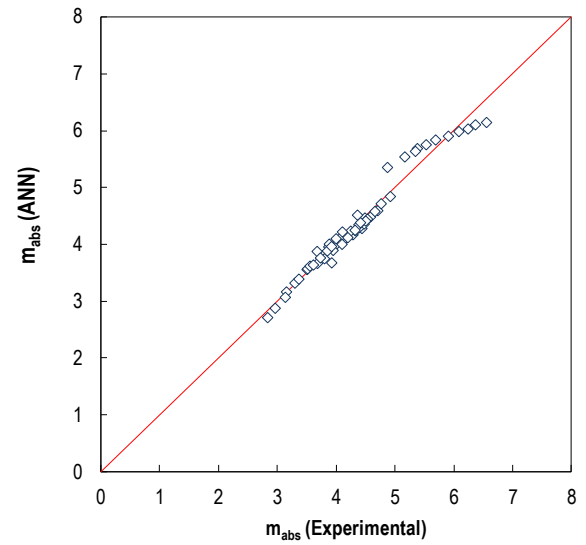
558 Figure 4. Structure of the neural network employed to predict the performance parameters of the  
 559 horizontal falling film absorber that uses an aqueous nitrate solution as a working fluid.

560

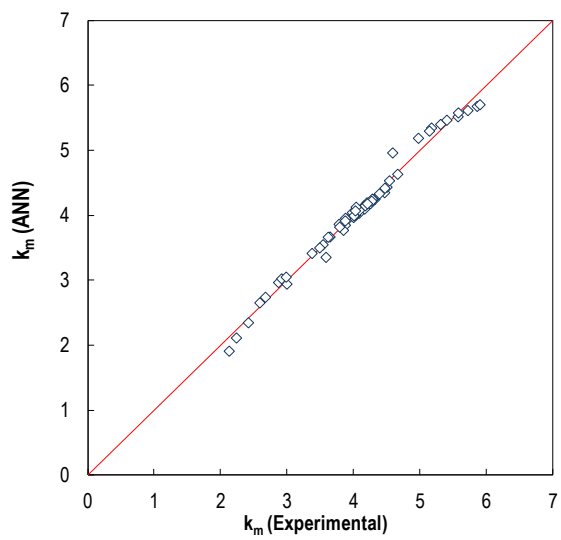
561



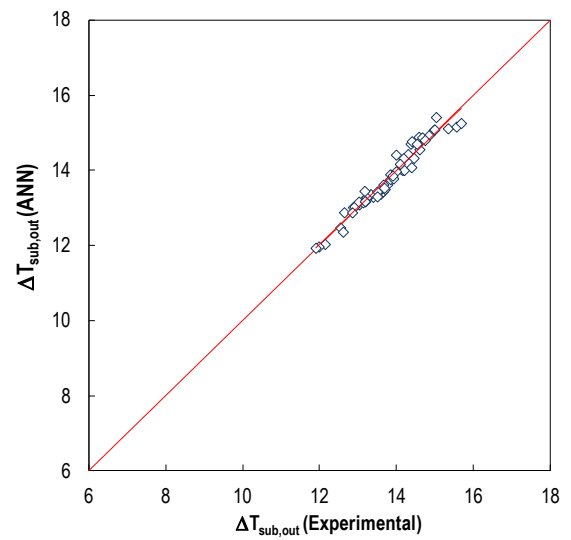
(a)



(b)



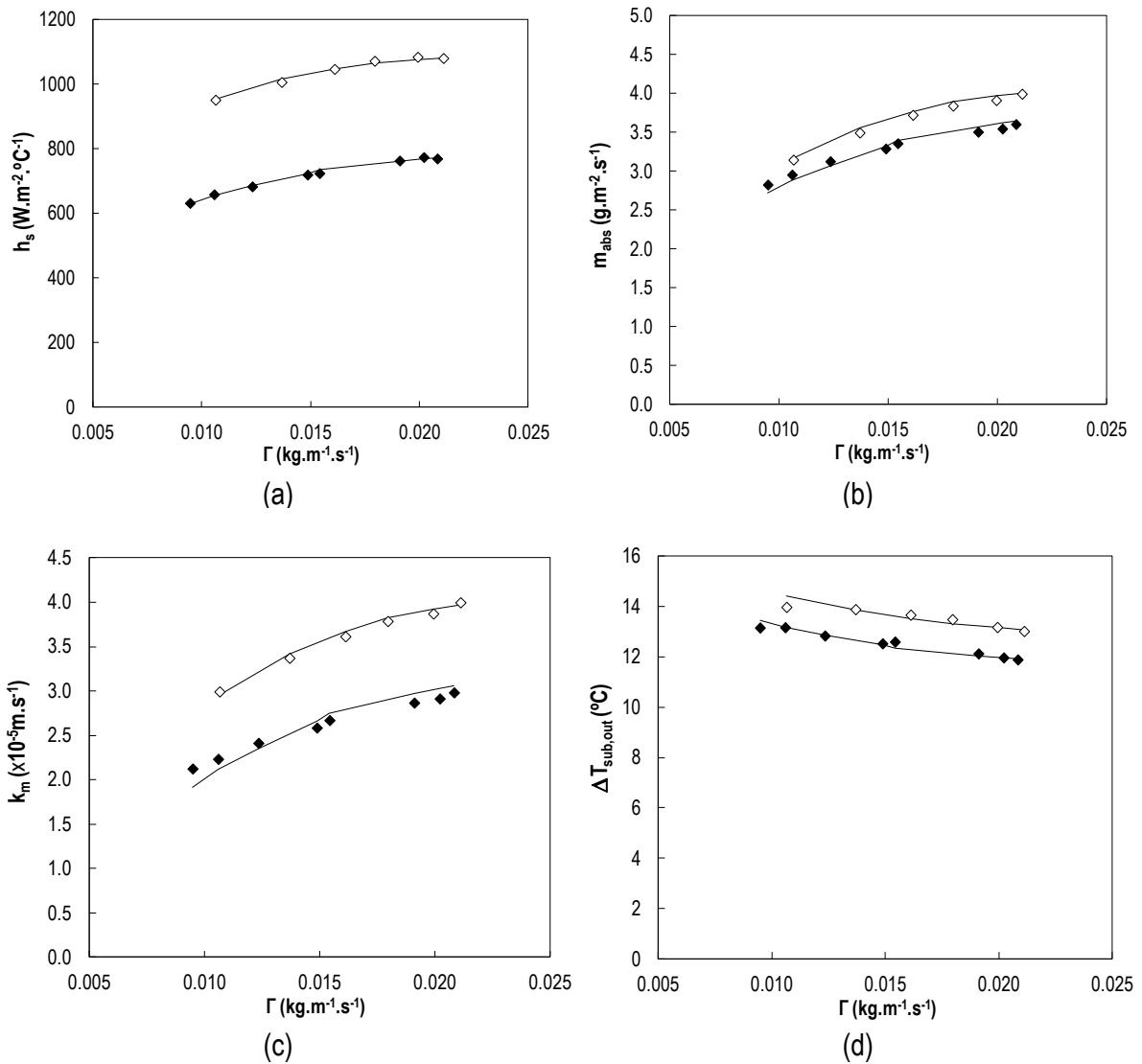
(c)



(d)

563 Figure 5. Comparison between experimental data and the values obtained using the ANN model (a)  
 564 Falling film heat transfer coefficient,  $h_s$ ; (b) Absorption mass flux,  $m_{abs}$ ; (c) Mass transfer coefficient,  
 565  $k_m$ ; (d) Degree of sub-cooling of the solution leaving the absorber,  $\Delta T_{sub,out}$ .

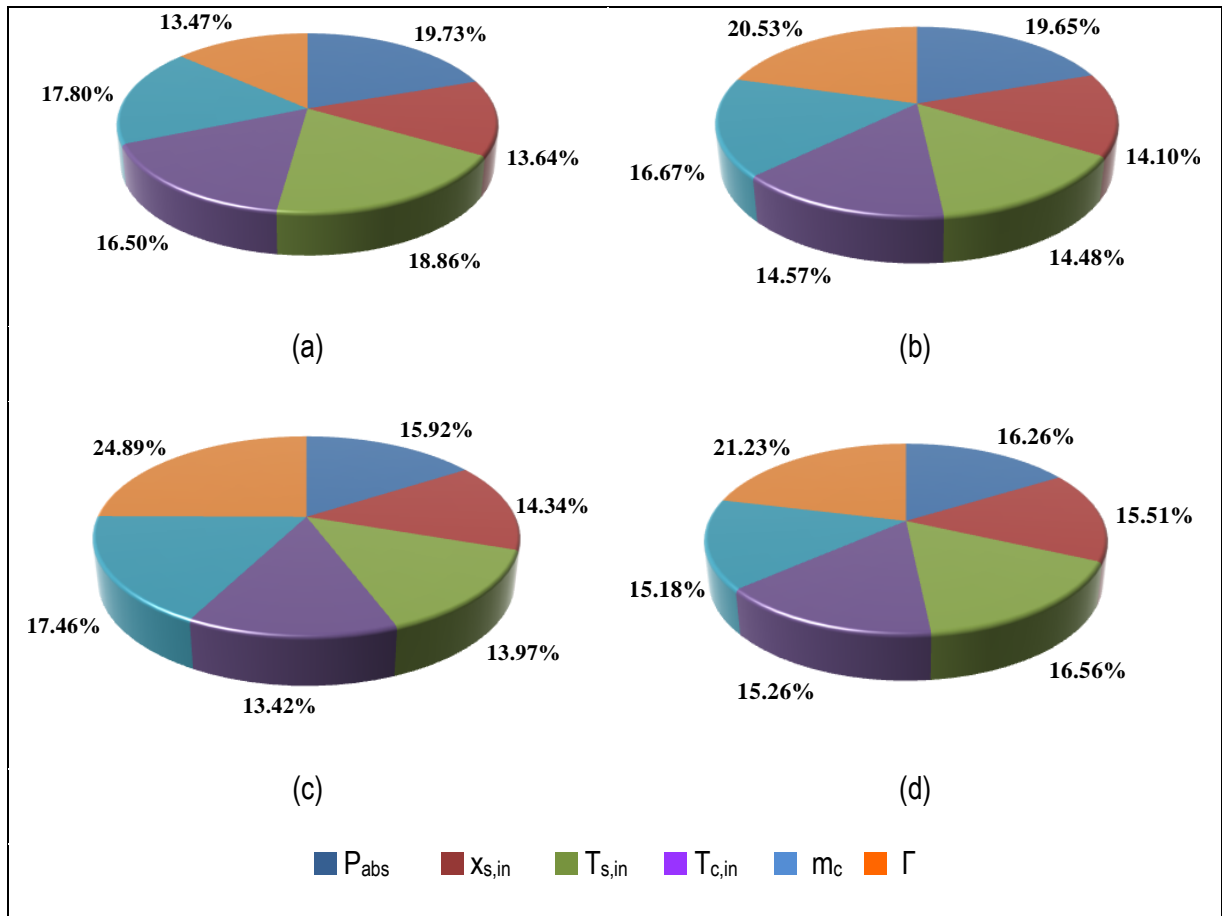
566



568

569 Figure 6. Validation of the ANN model to predict the absorber performance parameters:  $\blacklozenge$  75%  
 570 (experimental data),  $\diamond$  82% (experimental data), \_\_\_ prediction by the neural network of: (a) Falling  
 571 film heat transfer coefficient ( $h_s$ ); (b) Absorption mass flux ( $m_{abs}$ ); (c) Mass transfer coefficient ( $k_m$ );  
 572 (d) Degree of sub-cooling of the solution leaving the absorber ( $\Delta T_{sub,out}$ ).

573



575 Figure 7. Relative importance (%) of the inlet variables on each one of the performance parameters  
 576 of the absorber: (a) Falling film heat transfer coefficient ( $h_s$ ); (b) Absorption mass flux ( $m_{abs}$ ); (c) Mass  
 577 transfer coefficient ( $k_m$ ); (d) Degree of sub-cooling of the solution leaving the absorber ( $\Delta T_{sub,out}$ ).

580 **Tables Caption**

581 Table 1. Weights and biases of the ANN model to predict the performance parameters of the  
582 horizontal falling film absorber.

583 Table 2. rmse and  $r^2$  parameters for the ANN model used for the horizontal falling film absorber.

584 Table 3. Slope and intercept statistical test.

585

586

587 Table 1. Weights and biases for the ANN model to predict the performance parameters of the  
 588 horizontal falling film absorber.

Hidden layer									
Weight Matrix ( $IW_{ji}$ )						Bias ( $b_{1j}$ )			
-15.3474	43.1751	37.4287	15.0731	-25.3140	39.152	-70.0893			
41.6522	0.0969	13.2400	-15.5765	14.1442	-0.8481	7.1959			
-1.3711	-0.674	0.5508	1.3897	-0.3482	-0.0102	-0.2131			
0.4072	1.7606	-1.8388	-0.3248	0.1481	-1.5220	-0.1545			
-5.1331	-1.9946	1.7932	-0.6573	-13.8820	-1.9034	-40.7141			
-1.9445	2.5227	1.5022	1.1478	-6.2838	-14.3789	-13.4683			
3.1148	5.2899	6.0414	8.8363	5.5466	8.4793	8.2982			
0.3912	14.2885	7.0517	8.3928	8.4764	13.6098	12.4825			
32.4550	3.4598	-82.0933	-5.5388	-77.5926	20.119	41.1858			
Output layer									
Weight Matrix ( $LW_{kj}$ )						Bias ( $b_{2k}$ )			
64.9502	182.8450	-521.7766	-204.2631	104.7731	-111.9695	199.2661	156.8972	-295.553	214.1182
0.8390	2.9389	-1.8251	-1.3573	-0.5997	-2.6249	-0.8077	-2.0161	-0.0665	-0.6629
0.7732	3.1975	-1.4863	-1.6778	0.6430	-4.8402	-1.9724	-3.3902	-0.2799	0.0420
0.5458	2.8476	-1.7919	2.2732	0.0820	-2.4784	2.6958	3.1648	-0.7091	3.4573

589

590

591

592

593 Table 2. rmse and  $r^2$  parameters for the ANN model used for the horizontal falling film absorber.

	$h_s$	$m_{abs}$	$k_m$	$\Delta T_{sub,out}$
rmse	1.183	0.020	0.013	0.025
$r^2$	0.9989	0.9683	0.9867	0.9543

594

595

596 Table 3. Slope and intercept statistical test.

	$h_s$	$m_{abs}$	$k_m$	$\Delta T_{sub,out}$
$m_{sup}$	1.0107	1.0642	1.0523	1.0829
$m_{inf}$	0.9819	0.9081	0.9505	0.8936
$b_{sup}$	21.3065	0.4123	0.2108	1.4691
$b_{inf}$	-13.4416	-0.2784	-0.2147	-1.1450

597